IOP Conf. Series: Materials Science and Engineering **1345** (2026) 012020 doi:10.1088/1757-899X/1345/1/012020

Experimental assessment of the parasitic thermal load on cryogenic envelope for superconductive cables

Giovanni Mangiulli[1*], Tommaso Botto[2], Pietro Corsaro[2], Stefania Farinon[3,4], Luca Davide Marocco[5], Umberto Melaccio[2], Laura Savoldi[1,3], Luca Sessarego[4]

[1] Department of Energy, Polytechnic of Turin, Italy
[2] ASG Superconductors, Genoa, Italy
[3] National Institute of Nuclear Physics, Genoa, Italy
[4] Department of Physics, University of Genoa, Italy
[5] Department of Energy, Polytechnic of Milan, Italy

*giovanni.mangiulli@polito.it

Abstract. In the context of the hydrogen economy, transporting liquid hydrogen (LH2), instead of the gaseous one, is considered appealing due to the maximization of the energy density. The liquefaction of hydrogen is, however, an expensive process as it requires cryogenic conditions, typically in the range 20 K - 30 K, depending on operating pressure. To maximize the economic revenue from the transfer of LH2, the combination with other technologies requiring cryogenic operation can be considered, such as the power transfer through superconductors. Accurately quantifying the parasitic thermal load affecting the cable typically housed in a cryogenic envelope, is critically important. The Envelope is typically made of coaxial corrugated tubes to ensure flexibility and resilience against thermal contraction, facilitating connections between terminals and joints positioned at specific intervals. This study assesses the parasitic load through the envelope through boil-off measurements, relying on the correlation between the parasitic heating and vapor generation rate from liquid cryogen. Liquid nitrogen is selected as the cryogen, for the sake of availability, safety and cost. A lumped model is used to describe the behaviour of the system. It turned out that the parasitic load is $\sim 2.1\frac{W}{m}$ at LN2 temperature. An extrapolation with the temperature range relevant for the LH2 operation results in +30% of the measured heat. These values match with the actual state of the art.

1. Introduction

Superconducting technologies are increasingly being applied across a wide range of fields. To fully harness the properties of superconducting materials, achieving cryogenic temperatures is essential [1]. Among the numerous applications of superconducting materials, one of particular significance is electric power transmission [2], [3], [4], particularly using magnesium diboride (MgB_2). Due to the critical temperature of this material, liquid hydrogen is an ideal coolant, as it operates at temperatures around 20 K for pressures exceeding 1 bar, which makes it highly suitable for maintaining the superconductivity of MgB_2. This approach offers the dual advantage of eliminating ohmic heating while simultaneously transporting a secondary energy carrier. To implement this solution, the superconducting cable must be contained within a flexible cryostat designed to allow the flow of liquid hydrogen. Consequently, it is crucial that the cryostat minimizes parasitic heat ingress from the external environment. A comprehensive thermal characterization of the various cryostats is therefore essential to ensure optimal performance. One fundamental principle for cryogenic thermal characterization is the measurement of boil-off rate, which offers several key advantages, including enhanced safety, ease of replicating the test facility, a high degree of maturity and reliability, and the use of a simple, steady-state thermodynamic model, that is

$$\dot{m} \cdot \lambda = Q \tag{1}$$

Whit $\dot{m}$ representing the mass flow rate of the boil-off gas, λ is the vaporization latent heat and Q is the total power absorbed by the cryostat. In 1992, Ohi et al. [5] published a thorough review of various boil-off configurations, exploring different rigid cryostat geometries. According to a 2004 study by Fesmire et al. [6], three NASA-developed devices based on ASTM standards C177, C718, and C745 can be identified. These devices differ in cryostat dimensions and internal component arrangements, yet all utilize liquid-nitrogen boil-off at 77 K. The first standardized procedure for rigid cryostat testing was published in 2013 as ASTM C1774, which continues to serve as the reference for thermal characterizations of rigid cryostats in cryogenics. In 2015, Fesmire et al. introduced new boil-off calorimetry systems conforming to ASTM C1774 (2013) [7]. Regarding flexible cryostats, the first research studies on their thermal characterization were initiated in 2004. During this period, Fesmire et al. developed a patent for a system designed to test thermal conductivity [8]. To evaluate these samples, the ASTM C335 procedure for piping systems can be applied, appropriately adapted for cryogenic temperatures. The test apparatus can operate in a boil-off mode for pipelines carrying cryogenic fluids: in this configuration, the heat loss is calculated by measuring the evaporated mass flow rate, which is driven by a minor elevation achieved by tilting the horizontal tube of a small angle. Alternatively, a continuous-flow method can be employed, where the heat leak is calculated based on equation (2).

$$\dot{m} \cdot c_p \cdot \Delta T = q' \cdot L \tag{2}$$

Where $\dot{m}$ is the mass flow rate of the liquid, c_p its specific heat and ΔT the temperature change across the system. The boil-off method remains the most widely used for both rigid and flexible cryostats due to its simplicity and is internationally recognized as the standard (ASTM C1774). Despite the high technological maturity in this field, significant challenges persist in developing standardized experimental procedures for flexible cryostats, for which there is currently no established protocol. Additionally, the proposed procedures for thermal characterization of flexible cryostats appear to be more complex in terms of spatial and instrumentation requirements. This article introduces an alternative approach to measure the parasitic heat ingress for a 20 m-long flexible cryostat for superconducting cables, which, according to the previously mentioned procedures, would require a significant amount of space. The cryostat under test is equipped with two approximately 1 m-long end fittings, each featuring a labyrinth designed to minimize conductive heat ingress at the terminations (Figure 1a) and is characterized by a 65 mm-inner diameter. The model employed provides a detailed description of both the terminations and the cryostat's thermal contributions, with an impact on the amount of evaporated gas. Subsequently, the test facility is designed, assembled, and a short test campaign is conducted. Finally, the results are discussed, and the parasitic heat value, expressed as $q'\left[\frac{W}{m}\right]$, is calculated from the model.

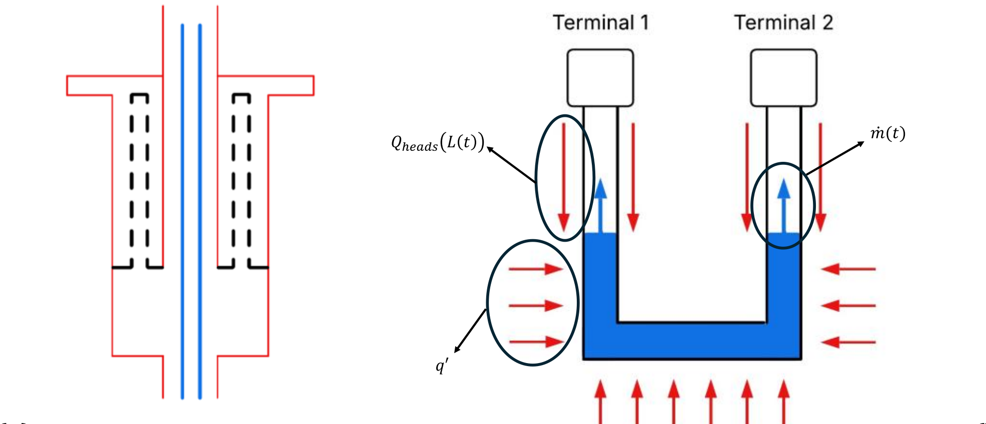

Figure 1. (a) Schematic of the end fittings of the 20 m-long characterized flexible cryostat. The dashed lines indicate the inner labyrinth used to reduce the end fittings' thermal contribution. (b) Scheme of the model associated to the characterization technique.

2. Methodology

The method used to characterize the cryostat is boil-off calorimetry. To accurately determine the boil-off rate for heat ingress calculations, a maintained height difference is necessary to facilitate natural vapor circulation, allowing the vapor to pass through a sensor for measurement. Following the approach used in existing facilities, such as the Cryostat-P100 [9], one can employ a minimally inclined horizontal run. However, due to the 20 m length of the cryostat and spatial constraints, a U-shaped configuration has been chosen (Figure 2). This more compact arrangement still provides sufficient elevation head to promote vapor exit. The model considered for parasitic heat measurement is the following:

$$\dot{m}(t_i) \cdot \lambda = q' \cdot L(t_i) + Q_{heads}\left(L(t_i)\right) \quad (3)$$

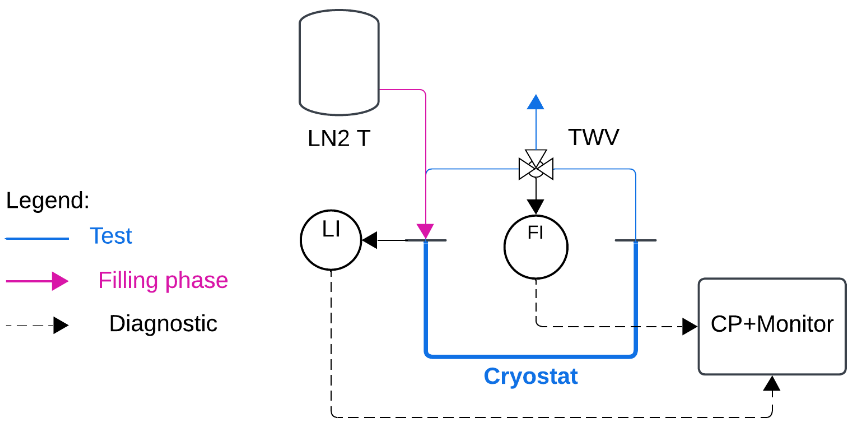

Figure 2. Layout of the test facility: FI-flow Indicator; TWV-Three Way Valve; LN2 T-Liquid Nitrogen Tank (dewar); LI-Level Indicator.

IOP Conf. Series: Materials Science and Engineering **1345** (2026) 012020 doi:10.1088/1757-899X/1345/1/012020

$$Q_{heads}\big(L(t_i)\big) = k_{ss} \cdot A_{ss} \cdot \frac{\Delta T}{\big(L_{tot} - L(t_i)\big)} \tag{4}$$

$$L(t_i) = L(t_{i-1}) - \frac{\dot{m}(t_i) \cdot \Delta t}{\rho_l \cdot A} \tag{5}$$

In Table 1 are summarized the different elements of the equations. The measuring of the parasitic heat, according to this model, consists of the direct measuring of the mass flow rate. The model scheme is summarized in Figure 1b. In the current model the calculation of heat transmitted through the end fittings (terminals) does not consider the labyrinth presence, which would decrease this contribution. This implies that the computed heat is a conservative value.

The test facility layout is shown in Figure 2: the test procedure consists of an initial transient cool-down and filling phase. Using a liquid-nitrogen dewar, the internal environment is initially cooled from approximately 300 K down to saturation, during which the injected liquid nitrogen rapidly vaporizes (chill-down phase [10]). Once saturation temperature is reached, the nitrogen remains liquid, and the cryostat fill is carried out under steady-state boil-off conditions. Once the cryostat has been filled with liquid nitrogen, the incoming heat load will cause the refrigerant to evaporate. The vapor exits through the two end fittings and is directed through a T-valve (labeled “TWV” in Figure 2) passing through a flow meter.

Table 1. Summary of the different symbols of the involved equations.

Symbol	Meaning
$L(t_i)$	Wet length of the cryostat at time t
Q_{heads}	Inlet heat from the end fittings labyrinth
k_{ss}	Thermal conductivity of the stainless steel
A_{ss}	Cross section of the annulus of the cryostat
Δt	Time interval of each data acquisition of mass flow rate
ρ_l	Density of liquid nitrogen at saturation condition for 1 bar
A	Section of the liquid nitrogen in the cryostat
L_{tot}	Total length of the cryostat (20 m)

Even if only a mass flow meter is necessary to measure parasitic heat, the initial value of the wet length at which data acquisition starts must be known. As consequence, a level probe has been used.

3. Experimental setup

The used probe is an American Magnetics Model 1700 Liquid Level Instrument while the mass flow meter is a TSI 5300 (Figure 3a). The level probe showed data in percentage form, so to start the data acquisition process with the mass flow meter, the 0% level must be reached, which

IOP Conf. Series: Materials Science and Engineering **1345** (2026) 012020 doi:10.1088/1757-899X/1345/1/012020

(a) 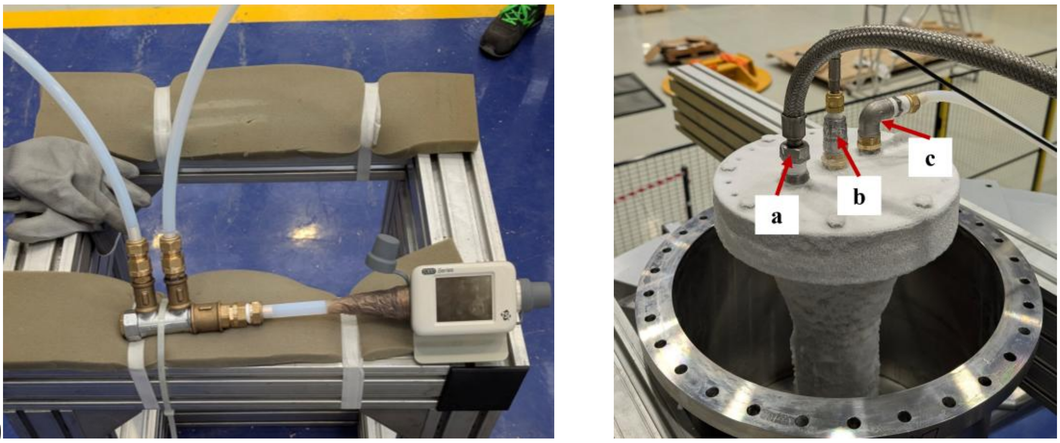 (b)

Figure 3. (a): TSI 5300 Mass Flow Meter with the T-valve and the two pipes from the end fittings. (b): Detail of one end fitting. (a)-transfer line; (b)-level indicator; (c)-boil-off gas collector pipe.

corresponds to 17.2 m. The flow data were initially recorded in standard liters per minute (SLPM) and then converted based on the temperature and pressure readings provided by the flow meter. To guarantee the typical U-tube configuration, two platforms have been used to keep the end fittings at a higher position and make the buoyancy effect work (Figure 4). From each terminal, the flow is directed to the mass flow meter by a tube. The two tubes and the mass flow meter are linked by a T-valve (Figure 3a).

Each tube has its own sealing assembly, characterized by a closure nut, an O-ring and an insulation layer by exploiting the metal's thermal contraction to avoid boil-off gas leakages. One of the two terminals has also the level probe installed and the direct link to the dewar through a transfer line (Figure 3b) while the other has two plugs to ensure the only boil-off gas flow. The whole test facility is shown in Figure 4.

4. Results and discussion

Two tests were performed in order to determine the average value and the uncertainty interval to

Figure 4. Test facility assembled with the two platforms.

characterize the cryostat and ensure the reliability of the results. Test 1 had a duration of 22 hours, while Test 2 was extended to 40 hours to observe a further reduction in the terminal heat-leak

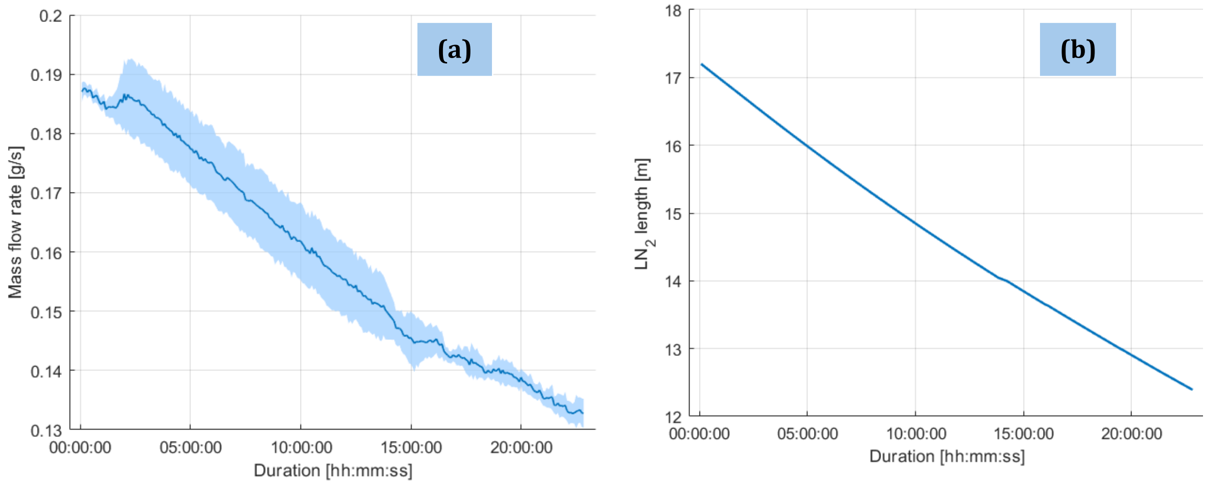

Figure 5. Average values of the measured mass flow rate and computed value of the wet length with equation (5): (a) Mass flow rate; (b) Wet length.

contribution and thereby isolate the cryostat's own parasitic load. The average value has been computed for the duration of the shortest test. The average mass flow rate (converted in g/s) and the wet length are reported respectively in Figure 5a and 5b.

The mass flow rate tends to decrease with time because of the increasing pressure on the free surface of liquid nitrogen due to the progressive level decrease: if pressure increases the latent heat of evaporation increases which implies that for the same parasitic heat, a lower amount of boil-off gas is generated. However, the used model tends to simplify the physical phenomenon in order to have an easier method to quantify the inlet heat.

If the wet length is known, end fittings heat is computed from equation (4). Finally, the parasitic heat can be determined from equation (3). The results of the average values during time are shown in Figure 6: it can be observed that the average value of the heat load is almost 2.1 W/m.

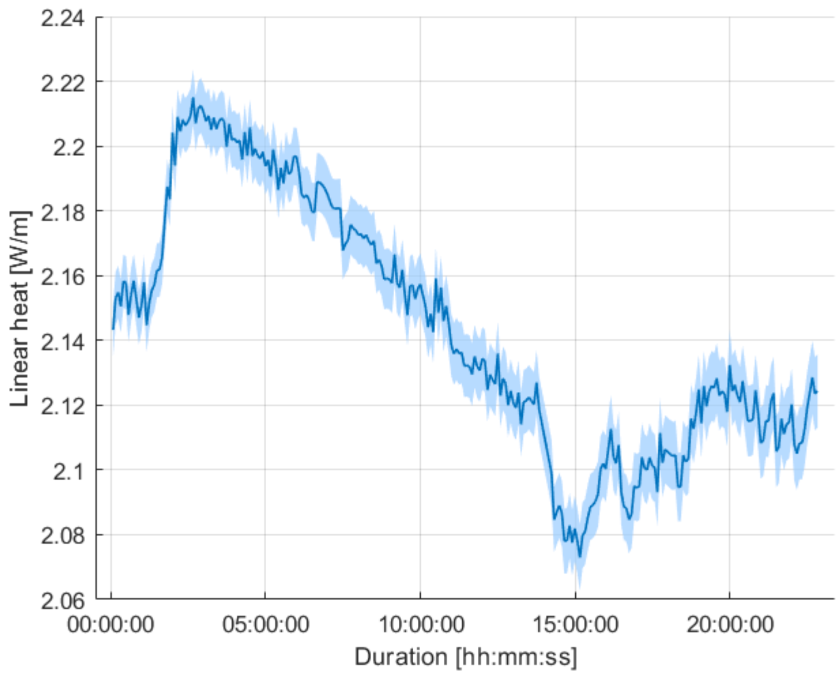

Figure 6. Average parasitic heat load on the flexible cryostat.

IOP Conf. Series: Materials Science and Engineering **1345** (2026) 012020 doi:10.1088/1757-899X/1345/1/012020

Considering that the characterization test was conducted at 77 K, while the cable's application requires operation at 20 K (the temperature of liquid hydrogen, LH2), it is necessary to extrapolate the effective heat load accordingly. To account for the vacuum chamber located between the inner and outer cryostats, an electrical analogy has been utilized for the Multi-Layer Insulation (MLI) region, based on the layer-by-layer model developed by McIntosh [11]. In this analogy, each layer is represented by two parallel thermal resistances, corresponding to radiation and conduction heat transfer mechanisms. The contribution of radiative heat transfer between concentric layers is described by the following equation:

$$q' = \frac{\sigma \cdot (T_{hot}^4 - T_{cold}^4)}{\pi \cdot D \cdot \left(\frac{1-\epsilon_{hot}}{\epsilon_{hot}} + 1 + \frac{1-\epsilon_{cold}}{\epsilon_{cold}}\right)} \tag{6}$$

Where σ is the Stefan-Boltzmann' constat ($\sim 5.67 \cdot 10^{-8} \frac{W}{m^2 \cdot T^4}$) and ϵ is the emissivity of the surface involved in the heat transfer which depends on the temperture of the surface. The correlation between emissivity and temperature is given by Chorowski [12]. The conduction contribution is given by the equation (7):

$$q' = \frac{2 \cdot \pi \cdot \mathrm{k_{MLI}(T)} \cdot \Delta T}{\ln\left(\frac{r_{out}}{r_{in}}\right)} \tag{7}$$

In equation (7) the term $k_{MLI}(T)$ is the Multi Layer Insulation (MLI) thermal conductivity, expressed by an empirical correlation in Eq. 8, the coefficients of which are reported by Hoffmann [13].

$$k_{MLI}(T) = a + b \cdot T^c \tag{8}$$

The effective heat load can be estimated by updating the cryogen temperature using appropriate radiation and conduction thermal resistances. This extrapolation indicates a parasitic heat increase of approximately 30%. The resulting effective parasitic heat values are consistent with those observed in commercial flexible cryostats for superconducting cables (~1-2.5 W/m) [14], [15], [16], [17]. However, a validation of the extrapolation method through an additional experimental campaign is required.

5. Conclusions and perspectives

In the present work, an alternative approach to characterize flexible cryostats based on the boil-off technique has been presented. Results are shown and are in accordance with the present state of the art. In order to reduce the interval of variability of results, more tests are required. Additional tests with a superconducting cable inside could be possible to be compliant with the final application of the cryostat to quantify an eventual additional load on the cryogen.

References

[1] Adams D Q et al. 2022 CUORE opens the door to tonne-scale cryogenics experiments *Prog. Part. Nucl. Phys.* **122**.

[2] Bracco M et al. 2025 Design of a Submarine 30-km MgB2 Cable for the Combined Transfer of 0.3 GWe and LH2 from Offshore Plants to the Ravenna Port *IEEE Trans. Appl. Supercond.* **35** 5400906.

IOP Conf. Series: Materials Science and Engineering **1345** (2026) 012020 doi:10.1088/1757-899X/1345/1/012020

[3] Savoldi L, Balbo A, Bruzek C E, Grasso G, Patti M and Tropeano M 2024 Conceptual Design of a SuperConducting Energy Pipeline for LH2 and Power Transmission Over Long Distances *IEEE Trans. Appl. Supercond*. **34** 5400805**.**

[4] Magnusson N et al. 2024 SCARLET – A European Effort to Develop HTS and MgB2 Based MVDC Cables *IEEE Trans. Appl. Supercond*. **34** 5400205.

[5] Ohi T 1992 Calorimetry by Boil-Off Measurement *Cryogenics* **27** 315–324.

[6] Fesmire J, Augustynowicz S, Heckle K and Scholtens B 2004 Equipment and Methods for Cryogenic Thermal Insulation Testing *Cryogenic Engineering Conf. (Anchorage, AK, USA, 2003).*

[7] Fesmire J E, Johnson W L, Meneghelli B J and Coffman B E 2015 Cylindrical boiloff calorimeters for testing of thermal insulation systems *IOP Conf. Ser.: Mater. Sci. Eng*. **101** 012056

[8] Fesmire J E, Nagy Z F and Augustynowicz S D 2004 Apparatus and Method for Thermal Performance Testing of Pipelines and Piping Systems US Patent 6,715,914 B1

[9] Fesmire J E 2016 Below Ambient and Cryogenic Thermal Testing *Adv. Cryog. Eng*. **61** 1463–1475.

[10] Kunniyoor K R, Govind R, Venkateswaran K and Ghosh P 2021 Liquid hydrogen pipeline chill-down: Mathematical modelling and investigation *Cryogenics* **118** 103324.

[11] McIntosh G E 1994 Layer by Layer MLI Calculation Using a Separated Mode Equation *Advances In Cryogenic Engineering* (Boston, MA: Springer).

[12] Chorowski M, Grzegory P, Parente C and Riddone G 2000 Experimental and Mathematical Analysis of Multilayer Insulation below 80 K LHC Project Report 385 (CERN).

[13] Hofmann A 2006 The thermal conductivity of cryogenic insulation materials and its temperature dependence *Cryogenics* **46** 815–824.

[14] Demko J A, Fesmire J E and Augustynowicz S D 2008 DESIGN TOOL FOR CRYOGENIC THERMAL INSULATION SYSTEMS *Cryogenic Engineering Conf. (Chattanooga, TN, USA, 2007)*.

[15] Demko J A, Duckworth R C and Roden M 2008 TESTING OF A VACUUM INSULATED FLEXIBLE LINE WITH FLOWING LIQUID NITROGEN DURING THE LOSS OF INSULATING VACUUM *Cryogenic Engineering Conf. (Chattanooga, TN, USA, 2007)*.

[16] Demko J A, Duckworth R C, Fisher P W, Gouge M J, Rey C M, Young M A, Lindsay D, Roden M, Tolbert J, Willen D, Træholt C and Thidemann C 2006 Testing of a Liquid Nitrogen Cooled 5-meter, 3000 A Tri-Axial High Temperature Superconducting Cable System *Cryogenic Engineering Conf. (Keystone, CO, USA, 2005).*

[17] Demko J A, Lue J W, Gouge M J, Stovall J P, Butterworth Z, Hughey R L, Lindsay D, Roden M, Sinha U 2002 Acceptance test and operation of the Southwire Company 30-m high-temperature superconducting cable cryogenic system *Cryogenic Engineering Conf. (Madison, WI, USA, 2001).*